

# Stellar Mixing and the Primordial Lithium Abundance

M.H. Pinsonneault<sup>1</sup>, G. Steigman<sup>1,2</sup>, T.P. Walker<sup>1,2</sup>, & V.K. Narayanan<sup>3</sup>

January 11 2001

## ABSTRACT

We compare the properties of recent samples of the lithium abundances in halo stars to one another and to the predictions of theoretical models including rotational mixing, and we examine the data for trends with metal abundance. We apply two statistical tests to the data: a KS test sensitive to the behavior around the sample median, and Monte Carlo tests of the probability to draw the observed number of outliers from the theoretical distributions. We find from a KS test that in the absence of any correction for chemical evolution, the Ryan, Norris, & Beers (1999) (hereafter RNB) sample is fully consistent with mild rotational mixing induced depletion and, therefore, with an initial lithium abundance higher than the observed value. Tests for outliers depend sensitively on the threshold for defining their presence, but we find a 10–45% probability that the RNB sample is drawn from the rotationally mixed models with a 0.2 dex median depletion with lower probabilities corresponding to higher depletion factors. When chemical evolution trends (Li/H versus Fe/H) are included in our analysis we find that the dispersion in the RNB sample is not explained by chemical evolution; the inferred bounds on lithium depletion from rotational mixing are similar to those derived from models without chemical evolution. Finally, we explore the differences between the RNB sample and other halo star data sets. We find that differences in the equivalent width measurements are primarily responsible for different observational conclusions concerning the lithium dispersion in halo stars. Implications for cosmology are discussed. We find that the standard

---

<sup>1</sup>Department of Astronomy, The Ohio State University

<sup>2</sup>Department of Physics, The Ohio State University

<sup>3</sup>Princeton University, Dept. Astrophysical Sciences and Observatory

Big Bang Nucleosynthesis predicted lithium abundance which corresponds to the deuterium abundance inferred from observations of high-redshift, low-metallicity QSO absorbers requires halo star lithium depletion in an amount consistent with that from our models of rotational mixing, but inconsistent with no depletion.

*Subject headings:* stars: abundances; cosmology: cosmological parameters; stars: rotation

## 1. Introduction

The primordial abundance of the light element lithium provides a crucial test of Big Bang nucleosynthesis (BBN); it is also an important diagnostic of standard and nonstandard stellar evolution theory. The detection of  ${}^7\text{Li}$  in halo stars by Spite & Spite (1982) opened up the prospect of the direct detection of the primordial lithium abundance. There have been a number of subsequent observational efforts which have produced a detailed picture of the distribution of halo star lithium abundances (Spite & Spite (1993); Thorburn (1994) (hereafter T94); Bonifacio & Molaro (1997); RNB; see also Ryan *et al.* (1996)). Primordial  ${}^7\text{Li}$ , as one of the four light nuclides produced in measurable abundance in standard BBN (the others being D,  ${}^3\text{He}$ , and  ${}^4\text{He}$  — see Olive, Steigman, & Walker (2000) for a review), provides a crucial consistency check in that all four nuclides are determined by the one free parameter of standard BBN — the baryon-to-photon ratio,  $\eta$ . Currently, the primordial deuterium abundance provides the best estimate of  $\eta$ . However, the BBN-predicted primordial lithium abundance which is consistent with the observationally inferred primordial deuterium abundance (and thus with our best estimate of  $\eta$ ) is actually *much* larger than the lithium abundance observed in halo stars. We show that theoretical models which include rotational mixing (and are required by the observed dispersion of halo lithium abundances) predict a primordial lithium abundance which is consistent, in the context of standard BBN, with the observed primordial deuterium abundance.

### 1.1. Stellar Models Compared with Earlier Data Sets

The interpretation of the halo star data requires knowledge of the stellar evolution effects which have influenced the surface abundance during the lifetime of the stars. In “classical” (*i.e.*, nonrotating) stellar models lithium is destroyed on the main sequence only in the presence of a deep surface convection zone; some pre-main sequence depletion will occur

for a wider range of masses. Such models predict only small amounts of lithium depletion for the hottest subdwarfs (effective temperature greater than about 5800 K) and for their Population I analogs (*e.g.*, Deliyannis, Demarque, & Kawaler (1990)). In the Population I case classical models make detailed predictions about lithium depletion which can be tested using data from open clusters with a range of ages. The open cluster data is in strong contradiction with the predictions of classical models. In particular, there is observational evidence for a dispersion in lithium abundance at fixed mass, composition, and age, and also for lithium depletion on the main sequence in stars with surface convection zones too shallow to burn lithium in the classical models (*e.g.* Balachandran (1995); Pinsonneault (1997); Jones, Fischer, & Soderblom (1999)). The rate of main sequence depletion is observed to decrease with age, and there are also strong mass-dependent depletion effects, none of which are predicted by the classical stellar models.

A number of physical mechanisms neglected in classical stellar models have been suggested as possible causes for the discrepancies. Rotational mixing is one attractive explanation since a range in initial rotation rates will produce a range in rotational mixing rates and the rate of rotational mixing would decrease with age as low mass stars lose angular momentum. Unfortunately, models of Population II stars cannot be subjected to the same stringent level of tests that can be performed for open cluster stars. The major unique signature of rotational mixing in the Population II context is therefore the presence of a *dispersion* in lithium abundance at fixed mass and composition. As a result, much of the theoretical and observational work on the subject has therefore focused on the existence and magnitude of dispersion in the Population II lithium abundances.

In a previous paper (Pinsonneault *et al.* (1999), hereafter PWSN) we computed the distribution of  ${}^7\text{Li}$  depletion factors expected from stellar models including rotational mixing. The distribution of depletion factors was compared with the largest uniform data set available, that of T94. We concluded that a combination of the observed dispersion in abundances, the relative depletion of the isotopes  ${}^7\text{Li}$  and  ${}^6\text{Li}$ , and the existence of a small population of highly depleted stars all argued in favor of the stellar depletion of lithium and we placed bounds of 0.2 – 0.4 dex on the  ${}^7\text{Li}$  depletion factor. In this paper we compare our theoretical calculations with the newer halo lithium data set of RNB.

The principal properties of lithium depletion in stellar models which include rotation can be summarized as follows. Rotation can induce mixing in the radiative interiors of stars leading to surface lithium depletion during the main sequence phase of evolution. This depletion due to rotational mixing is in addition to surface lithium depletion during the pre-main sequence and (in the case of cool stars) main sequence evolution. The degree of rotational mixing depends on the angular momentum content and its evolution so that a

range of pre-main sequence rotation rates will produce a range of lithium depletion factors, in the sense that rapid rotators experience more mixing and lithium depletion than do slow rotators. There is compelling evidence from the Population I data for main sequence lithium depletion as well as for a dispersion in lithium abundance at fixed mass, composition, and age; rotational mixing naturally explains this pattern. PWSN found that halo star models experience systematically less lithium depletion than do solar abundance models for the same sets of initial conditions.

The distribution of lithium depletion factors depends on the distribution of initial conditions, which can be inferred for young Population I clusters. The distribution of pre-main sequence rotation rates needed to reproduce the rotation data in the Pleiades cluster produced a degree of dispersion which is correlated with the absolute amount of  ${}^7\text{Li}$  depletion. Since the majority of young stars have similar rotation rates, the majority of stars will experience similar  ${}^7\text{Li}$  depletions. There is, however, a subpopulation of rapid rotators that are predicted to experience higher  ${}^7\text{Li}$  depletion. Comparison with the T94 data set led to a range of 0.2 – 0.4 dex in the inferred stellar depletion (PWSN). When combined with an observed “Spite plateau”  ${}^7\text{Li}$  abundance of  $2.25 \pm 0.10$  (on the logarithmic scale where  $H = 12.0$ ), this yielded a primordial  ${}^7\text{Li}$  abundance in the range of 2.35 – 2.75. We emphasize that the PWSN models have the following overall properties: in contrast to a simple gaussian distribution of abundances there is a distribution with a core whose dispersion is dominated by observational errors, along with a subpopulation (of order 1/5 of the sample) with moderately higher depletion factors, and a smaller population of (order 2-3% of the sample) with large depletion factors. These features will prove important in our comparison with newer halo star data of RNB.

## 1.2. New Results from RNB

The PWSN conclusions have recently been challenged by RNB using data from a high precision study of lithium abundances in a smaller, albeit still significant, sample of halo stars. They obtained both a lower absolute observed abundance (2.11) and a significantly reduced error estimate and dispersion. They attributed the residual dispersion to chemical evolution (e.g. the observed spread in  $\text{Li}/\text{H}$  in their view is caused by differences in post-BBN lithium production correlated with the range in  $\text{Fe}/\text{H}$ ). They argue that their data set *requires* stellar depletion be minimal. In recent papers (Ryan *et al.* (2000), Suzuki, Yoshii, & Beers 2000) the RNB results have been used to argue that the primordial lithium abundance is below their observed value in very metal-poor stars as a result of galactic production. In this paper we compare our models with this new data set and we also compare the RNB

data set with other studies. We begin by comparing the data set of RNB with the theoretical distributions of PWSN in section 2. We analyze the dispersion and chemical evolution trends in section 3 and compare the RNB and T94 data sets in section 4. Our conclusions concerning the primordial abundance of lithium and its consequences for cosmology are found in section 5.

## 2. Comparison of the Models with the Data

The RNB sample does have a dispersion in excess of their observational errors. RNB attribute this excess dispersion to chemical evolution. We will begin by comparing the RNB data to theory without any chemical evolution detrending; we consider both the reality of any trend with metallicity and its impact on the inferred lithium abundance in section 3. We note here that none of the overall conclusions of the comparison between data and theory in this section are dramatically modified by the treatment of chemical evolution effects (see section 3.) Furthermore, an analysis of the models without metallicity detrending provides the least model-dependent constraint on the degree of rotational mixing.

Differences in stellar rotation rates will produce differences in the degree of rotational mixing, so excess dispersion can be a signature of stellar depletion. However, the distribution of stellar rotation rates is needed in order to predict the distribution of stellar lithium depletion factors. Stellar models with rotation must also account for angular momentum loss from a magnetic wind and internal angular momentum transport. Finally, the degree of mixing for a given angular momentum distribution must be specified (see PWSN for a more detailed description.)

As discussed in PWSN, rotation data in young open cluster stars is our best current guide to the initial conditions that might be applicable to halo stars. The majority of young stars are slow rotators with similar rotation rates; these stars will have almost uniform depletion and very little internal scatter. About 15% of young stars are rapid rotators, including a subpopulation (about 3%) of very rapid rotators. This will produce a tail of overdepleted stars in the distribution. There are unavoidable observational selection effects which may influence the inferred distribution of rotation velocities. For example, very slow initial rotators would only have upper limits to their rotation velocity, so it is difficult to estimate how many stars should be underdepleted compared to the median. There are occasional claims of pre-MS stars with very long periods, and this might explain the occasional halo star above the lithium plateau. At the other end, the rapid rotator tail is subject to Poisson noise — the fastest spinner in the Pleiades is at 140 km/s and the second fastest is at 90 km/s. So the very far tail of the underdepleted stars is difficult to pin down. However, the behavior

of the peak of the distribution is not sensitive to these details. This provides justification for our including the one upper limit lithium abundance in the RNB sample and considering those outliers below, but not above, the median in our tests of the models.

We can empirically constrain the angular momentum loss and transport properties by comparing different classes of theoretical models to stellar observations as a function of mass and age. Angular momentum transport and mixing by hydrodynamic mechanisms are included in the models. We calibrate the mixing by requiring that a solar model reproduce the solar lithium depletion at the age and rotation rate of the Sun. However, we have no direct information on the solar initial conditions; because angular momentum loss scales as  $\omega^3$ , stars with a wide range of initial rotation rates end up with similar rotation rates at old ages. In PWSN, we considered three solar calibrations (s0, s0.3, and s1) which correspond to three different overall normalizations for the stellar lithium depletion. The s0 case assumes that the Sun was initially a rapid rotator, so the typical star will experience much less depletion than the Sun; the s0.3 and s1 cases correspond to assuming the Sun is more typical and the overall expected stellar depletion is therefore larger.

The Pinsonneault, Deliyannis, & Demarque (1992) depletion factor of 10 from rotational mixing came from the assumption that the Sun was a typical star; furthermore, these early models did not include a saturation of angular momentum loss for rapidly rotating stars. The current generation of models is in significantly better agreement with more recent measurements of stellar rotation rates, which both permits us to infer the distribution of rotation rates and to rule out depletion factors as large as the 1992 values.

There will be two principal differences between rotationally mixed and standard models that can be directly tested with the halo star lithium data. The internal range in rotation among slow rotators will produce an increase in the dispersion around the sample median relative to the observational errors; and the rapid rotators will be overdepleted relative to the median. We therefore apply two statistical tests to the data. We compare the cumulative distribution of stars to theoretical distributions anchored at the median abundance of the sample using a KS test. This test allows us to measure the constraints on stellar depletion from the tightness of the bulk of the halo lithium plateau stars.

We also applied both a simple analytical model and Monte Carlo simulations to test the probability of drawing the observed number of outliers from the theoretical simulations. For a given distance below the median there is a probability that any given star in the theoretical distribution will lie at or below that abundance ( $P_0$ ). For a sample of size  $N$ , the probability that there will be a given number  $I$  of stars below such a threshold is  $S_I P_0^I (1 - P_0)^{N-I}$  where  $S_I$  is the number of states capable of producing a given number of outliers. For  $I = 0, 1, S_I = 1, N$  respectively; it is straightforward if tedious to compute the number of accessible

states for more outliers. We used Monte Carlo simulations to check for the cases with larger numbers of outliers.

We also compare to a Gaussian distribution of errors. This permits us to test for the possibility that the excess dispersion arises from a global underestimate of the observational errors and to quantify the relative agreement of models with and without stellar depletion.

## 2.1. Comparison with the Cumulative Distribution

We convolved the theoretical distributions for the s0, s0.3, and s1 cases of PWSN described above with gaussian observational errors of 0.035 dex (see Section 4 for our determination of the observational errors). In Figure 1 we compare the cumulative RNB distribution with these three models and a Gaussian distribution of errors. The s0, s0.3, and s1 models have median depletion factors of 0.18 dex, 0.32 dex, and 0.50 dex respectively; on the RNB abundance scale these would correspond to initial abundances of 2.29, 2.43, and 2.56 respectively. Despite the very different depletion factors, all of the models have similar properties in the core of the distribution. Only the s1 case, with a high median stellar depletion of 0.50 dex, predicts a core broader than the observed distribution. Gaussian errors alone cannot reproduce both the tightness of the core and the presence of outliers in the sample.

KS tests applied to this distribution indicate that there is, respectively, a 60%, a 25%, and a 5% chance that the s0, s0.3, and s1 cases could be drawn from the same distribution as the data; by comparison the Gaussian has an 86% chance of being drawn from the same distribution as the data. We conclude from this test, which is primarily sensitive to the behavior of a sample around the median, that only high depletion factors are problematic — although even the highest depletion case is only excluded at the 95% level. This confidence level is too low to absolutely rule out a model. There is thus no contradiction between mild stellar depletion from rotational mixing and the presence of a core of halo lithium abundances with small internal scatter. This data suggests that the internal dispersion in the core is primarily caused by observational error, and furthermore that an underestimate of the observational errors is not responsible for the excess scatter in the data. At the same time, it also provides no support for depletion factors at or above the 0.5 dex level.

## 2.2. Number of Outliers

Inspection of Figure 1 reveals that the theoretical distributions predict more overdepleted stars than are present in the data set, but that there are more overdepleted stars

in the sample than are predicted by the observational errors (compare the solid and dotted curves). Because of the small number of stars (23) in the sample, and the even smaller number of outliers expected in the sample (3 –– 7), we believe that only tentative claims can be made about the consistency (or lack thereof) of modest depletion factors with the data. The basic issue is simply that the expected number of outliers in the rotational mixing models is small for a sample of 23 stars, which makes the conclusions subject to Poisson noise.

As an illustration, consider the different distributions in Figure 1. The tail of the observed distribution up to an abundance of 2.0 corresponds to three overdepleted stars; it is clearly inconsistent with the expectation from observational errors, since abundances this low are formally three  $\sigma$  or more below the median and therefore very unlikely in a sample of 23 stars. The highest depletion case predicts more stars more than 0.1 dex below the median (7) than are observed (3). However, the sample is so small that the specific statistical conclusions depend sensitively on where the threshold for defining an outlier is defined. If the threshold is defined at 2.01 (just above two of the three overdepleted stars), then the expected fraction of outliers relative to the data is minimized and there is a 45% chance of drawing the observed number of stars relative to the s0 case and less than a 0.1% probability of seeing as many as three outliers from observational errors alone.

However, there is a gap in the sample between abundances of 2.00 and 2.06; if an outlier is defined as being at or below 2.05 the expected outlier fraction is increased and the observed outlier fraction is the same. In this case there is a 10.6% chance of drawing the data from the minimally depleted s0 distribution and an 11.4% chance of seeing as many as three outliers from observational errors. Similar fluctuations arise from excluding the one upper limit from the sample or clipping the tail of the theoretical distribution. We therefore consider a range of probabilities from the most stringent (counting all stars more than 0.06 dex below the median as outliers) to the least stringent (counting all stars more than 0.10 dex below the median as outliers.)

The numbers in parenthesis after the listed fractional probabilities in the second and third columns of Table 1 are the expected number of outliers if we set the threshold for defining one at less than 2.06 or less than 2.01 respectively. The actual number of outliers is three below 2.01 or below 2.06, *e.g.*, there are no stars between 2.00 and 2.06. The probabilities for the Gaussian are for having three or more outliers; the probabilities for the other three cases are for having three or fewer outliers. Because of sparse sampling there is a range of possibilities for defining what an outlier is. The closer the cut is to the median, the larger the number of expected outliers; this favors the no-depletion case because there are more outliers than expected, but disfavors the stellar depletion case because there are

fewer outliers than expected.

If we exclude the one upper limit (G186-26), the minimum/maximum probabilities for the s0 case drop to 5.5% and 24.8% respectively for two outliers out of 22 stars. Ryan *et al.* (2001) have argued that the rare ultra-lithium depleted stars are binary merger products, and that they should therefore be excluded from samples of this type. In support of this they note that there is a large difference in abundance between the ultra-depleted stars (of order 5%) and others and that the fraction of overdepleted stars is very high in intermediate metal abundance stars which are hot enough to be plausible blue straggler candidates.

We first note that Ryan *et al.* (2001) does not establish a causal link between high lithium depletion and binary merger products; in fact, the authors argue that excess lithium depletion may be the sole indicator of such processes. The fraction of highly depleted stars in some clusters, such as M67 (Jones, Fischer, & Soderblom (1999)) is significantly higher than the norm, which could indicate at minimum that there is more than one cause for strong lithium depletion. Excluding stars that do not fit an expected pattern also amounts to an effective prior on the sample statistics. If highly depleted stars are *a priori* excluded from lithium samples then the highly depleted stars predicted by theoretical models should also be removed when doing statistical comparisons. If we remove the observed upper limit and the upper 5 % of depletion factors from the theoretical models on the grounds that they are rejected from samples of lithium abundances, we recover the same (or higher) probabilities as we infer from including the one upper limit in the sample. Therefore, in this and subsequent tests we retain the entire sample for statistical comparisons.

In contrast to the behavior around the sample median, the number of outliers sets stronger constraints on stellar depletion. The highest depletion case of 0.5 dex is ruled out at the 95% confidence level even if we use the most generous definition of what constitutes an outlier; this is a considerably stronger test than a similar confidence level for a KS test. The Gaussian error model has severe difficulty reproducing the observed number of outliers; it is excluded at the 90% confidence limit 0.05 dex below the median and at higher than a 99.9% confidence level 0.10 dex below the median. Formally, a model with 0.13 dex depletion would provide the best fit to the outlier fraction. The 0.32 dex depletion case is not formally excluded, but it is certainly disfavored by the present data set.

We can set some rough bounds on stellar depletion based on the RNB data sample without considering the effects of chemical evolution (discussed in Section 3) or possible systematic differences in equivalent width measurements (see Section 4.) Stellar depletion at the 0.1 dex level is fully consistent with the data. Models with depletion as high as 0.5 dex are less than 5% probable, while models with no depletion are less than 10% probable. PWSN compared the same models with the full T94 data set and concluded that stellar depletion

at the 0.2 dex level provided the best fit to the dispersion in the T94 data set; a range of 0.2 to 0.4 dex depletion was the result of several different diagnostics of stellar depletion including the presence of highly depleted stars and  ${}^6\text{Li}$  to  ${}^7\text{Li}$  ratio measurements and limits. The base RNB data set provides a lower central value for depletion; but because of the small sample size the bounds on depletion are actually widened relative to the conclusions of PWSN. In the next sections we consider other effects, and will return to our final estimate of the primordial lithium abundance in section 5.

### 3. Trends with Metal Abundance

The dispersion in the RNB sample exceeds their quoted observational errors; as we have shown above it is consistent with the theoretical predictions of mild rotational mixing. However, RNB concluded that the excess dispersion in their sample could be explained instead by post-BBN galactic production of lithium. As evidence for this they performed fits of lithium versus iron adopting for the functional form a fit which is a power-law in Li/H versus Fe/H:  $\log(\text{Li}/\text{H}) = \log(\text{Li}/\text{H})_P + a[\text{Fe}/\text{H}]$ , where  $[\text{Fe}/\text{H}] \equiv \log(\text{Fe}/\text{Fe}_\odot)$ .

Although this form may provide a good fit to the data over a limited range in metallicity, it certainly cannot describe the evolution of an element whose BBN abundance is expected to provide the dominant contribution to its halo abundance. To account for a significant BBN component along with a chemical evolution component that may scale linearly with the iron abundance (see for example Ryan *et al.* (2000)), the fitting function should be of the form  $\text{Li}/\text{H} = (\text{Li}/\text{H})_P + b(\text{Fe}/\text{Fe}_\odot)$ . Since post-BBN, early galactic production of lithium may be dominated by cosmic ray nucleosynthesis which depends more on the oxygen than the iron abundance, Ryan *et al.* (2000) also considered the consequences of an increasing oxygen abundance at low iron abundance. In this case a linear fit to lithium as a function of oxygen would take the form  $\text{Li}/\text{H} = (\text{Li}/\text{H})_P + b(\text{Fe}/\text{Fe}_\odot)^{0.7}$ . They found significant slopes ranging from  $4.0 \times 10^{-9}$  to  $1.8 \times 10^{-8}$  (in the *linear* iron – *linear* lithium plane) and ranging from  $0.9 \times 10^{-9}$  to  $3.4 \times 10^{-9}$  (in the *linear* oxygen – *linear* lithium plane) on the assumption that the controversial claims of very high oxygen abundance at low iron abundance are correct (Israelian, Garcia-Lopez, & Rebolo (1998); Boesgaard *et al.* (1999); but see also Fulbright & Kraft (1999), King (2000)). Although we obtain somewhat smaller slopes, we will show that the most important feature of these chemical evolution fits is that they do not explain the outliers seen in the RNB sample. Therefore, in contrast to RNB, we find that chemical evolution cannot account for the excess dispersion observed in their sample.

There are several issues which effect the quantitative fits for the possible early (low-

metallicity) evolution of lithium. For example, the fits depend on the adopted stellar metallicities and RNB included two sets of metallicity estimates. A literature value was taken from Ryan & Norris (1991), Ryan, Norris, & Bessel (1991), Carney *et al.* (1994), and (for one star) Beers, Preston, & Shectman (1992). There was also a 1 angstrom resolution estimate directly obtained by RNB for 21/22 detections in their sample. Since no error estimates are quoted in the paper, we estimated them in two ways. The rms difference between the two sets is 0.14 dex, consistent with a  $1\sigma$  error of 0.1 dex in each. This is also consistent with the error estimates in the primary sources used by RNB for the “literature” values. Furthermore, there is a zero-point difference of 0.13 dex between the literature and RNB metallicities, in the sense that the RNB values are higher. This different metallicity zero-point contributes to the range in the inferred chemical evolution slopes, in the sense that the slope inferred from the RNB metallicities is smaller than that obtained with the literature metallicities. Because the corrections to the lithium abundances are small, only in the literature case does the error in the metallicity have an impact on the overall dispersion (raising  $\sigma$  from 0.035 to 0.040 in the most extreme case.)

In addition, the RNB literature metallicities have an embedded effect that produces a significant component of the higher slope. Two of the sources — Ryan & Norris (1991), Ryan, Norris, & Bessel (1991) — are systematically 0.15 dex lower than Carney *et al.* (1994) because of a difference in the assumed solar iron abundance. The Ryan, Norris, & Bessel (1991) abundances were corrected to the Carney *et al.* (1994) scale, but the Ryan & Norris (1991) values were not; RNB also did not use RN91 or Carney when there was an abundance from Ryan, Norris, & Bessel (1991). To test for the importance of this effect we used the same primary sources, but corrected Ryan & Norris (1991) to the Carney *et al.* (1994) scale. We then averaged multiple measurements weighted by their respective errors. This reduces the rms scatter compared with the RNB 1 A metallicities by 25 percent, and the slope also drops by 25 percent. The direct  $1\sigma$  error in  $[\text{Fe}/\text{H}]$  is 0.08 dex. We therefore conclude that half of the difference between the literature and RNB abundances is caused by the combination of data from different sources in the RNB literature values and the other half is the metallicity zero point. We use the published literature RNB data for comparison with other papers that have used this data; we believe that the homogeneous RNB metallicities are a better choice for chemical evolution studies.

In Table 2 we show the data we used. The abundance errors were estimated by adding in quadrature the  $T_{\text{eff}}$  error, the RNB slope of 0.065 dex per 100 K, and the RNB equivalent width error in the linear curve of growth approximation. We obtain an average sample error of 0.036 dex rather than the RNB value of 0.032 dex; we have not been able to trace the origin of the latter number in the RNB paper. The T94 abundances have been converted to the RNB temperature scale using the temperature correction above; the T94 errors were

estimated from the T94 equivalent width errors and the temperature errors as described above. The average T94 error is 0.06 dex; we defer a discussion of the T94 data to section 4.

We considered two sets of metal abundances and two fitting functions in  $T_{\text{eff}}$  (linear and power law), for four basic cases. As already noted by RNB, much of the slope comes from three outliers in the sample; we therefore repeated the analysis for all four sets with the same outliers excluded as discussed in RNB. In Table 3 we present the eight sets of results. The cases are identified in column 1; the first four include outliers and the last four do not. The cases starting with L use the RNB [Fe/H] metal abundances which yield a low slope; the cases starting with H use the literature [Fe/H] values which yield a high slope. The cases ending with L are linear fits and the cases ending with P are power law fits. The zero-point and slope of the different fits are in columns 2 and 3. The median abundance corrected to zero metal abundance and both the predicted and actual residual dispersion are given in columns 4 to 6. The different cases are illustrated in Figures 2 and 3.

There are two important conclusions to be drawn from this exercise. First, the chemical evolution slopes are sensitive to *all* of the assumptions in the models, with a wide range of slopes possible. Second, detrending the data in the linear Li versus Fe plane does not bring the outliers onto the mean trend. In all cases the formal dispersion of the detrended samples are larger than the estimated errors. This can be traced directly to the presence of outliers whose lithium abundance differs significantly from the sample mean. Intuitively this can be easily understood; because the absolute metal abundances of the stars are small, there is little room for a significant chemical evolution correction. There are three stars noted as outliers in the RNB chemical evolution analysis: CD -24 17504 ([Li]= $1.97 \pm 0.033$ ,  $4.2\sigma$  below the mean); BD +9 2190 ([Li]= $2.0 \pm 0.042$ ,  $2.6\sigma$  below the mean); and CD -71 1234 ([Li]= $2.20 \pm 0.025$ ,  $3.6\sigma$  above the mean). In the linear fit to the literature iron abundances these three stars are respectively  $2.4\sigma$  below,  $2.3\sigma$  below, and  $2.0\sigma$  above the mean; for the linear fit to the RNB iron abundances the same stars are respectively  $3.3\sigma$  below,  $2.3\sigma$  below, and  $3.8\sigma$  above the mean. There is also the upper limit in G186-26, making a total of 4/23 outliers *regardless of the presence or absence of chemical evolution detrending*. Similar results apply to the power-law fits.

We have not performed chemical evolution fits for our rotationally mixed models because it is not a well-posed problem for such a small sample of lithium abundances; a metallicity-dependent distribution of stellar depletion factors needs to be convolved with a mean chemical evolution trend. From PWSN, we can anticipate that the contribution of a range of metallicities to the dispersion will be small and difficult to detect in a sample of this size.

### 3.1. Comparison of Theory and Observation Including Chemical Evolution Detrending

Table 3 presents the results of KS and outlier test comparisons of the models and data under different chemical evolution detrending scenarios. We have used the same theoretical models as in section 2. As noted in Table 3, the additional observational errors from the uncertainty in lithium production does not significantly impact the overall observed error. Because the various fits yield similar conclusions, in Figure 4 we show only the most probable of these cases. The observational data in in Figure 4 is the cumulative distribution of [Li] from the linear fit to the RNB metal abundances, corrected to zero metal abundance. We compare this data set to a gaussian with  $\sigma = 0.04$  dex and the same three theoretical distributions as in Figure 1. The qualitative trends are similar to those obtained with the base RNB data.

The five cases considered are no chemical evolution; low slope, linear Li-Fe (LL), low slope, power law Li-Fe (LP), high slope linear (HL), high slope power law (HP). The first three columns are the probabilities of drawing the data from the theoretical s0, s0.3, and s1 distributions. The no evolution case is evaluated at 0.1 dex below the median; the other cases are smoother and are evaluated in 0.01 dex increments between 0.05 and 0.1 dex below the median and averaged. The second set of three columns are the KS test probabilities for the same cases and theoretical distributions.

In Table 5, we give both the zero points and inferred primordial abundances for the different cases on the RNB abundance scale; we argue elsewhere that these should be adjusted up by 0.1 dex because of systematic model atmosphere/temperature scale effects.

### 3.2. Chemical Evolution Implications for ${}^6\text{Li}$

If, indeed, the abundance of lithium is evolving at very low-metallicity as RNB suggest, the most likely source of post-BBN lithium is from cosmic ray nucleosynthesis (Reeves, Fowler, & Hoyle (1970)). One consequence of CRN is the concomitant production of  ${}^6\text{Li}$  along with  ${}^7\text{Li}$  resulting in comparable amounts of post-BBN production of both isotopes. At very low-metallicity the lithium isotope production is dominated by  $\alpha - \alpha$  fusion (Steigman and Walker 1992) leading to a 7/6 production ratio of  $R_{76} \approx 1.6$  (Kneller, Phillips, and Walker 2000). At higher metallicity this ratio decreases slightly to  $R_{76} \approx 1.5$  (Steigman and Walker 1992; Kneller, Phillips, and Walker 2000). As a result, the  ${}^6\text{Li}/{}^7\text{Li}$  ratio provides a means to test the RNB hypothesis that the lithium abundance is increasing at a noticeable rate in the early Galaxy at very low metallicity ( $[\text{Fe}/\text{H}] \lesssim -2$ ). If the observed lithium

abundances (without allowance for depletion by rotational mixing) are fit to a metallicity relation of the form  $\text{Li}/\text{H} = a + bx$ , where  $a \equiv (\text{Li}/\text{H})_P$  and  $x$  is either  $\text{Fe}/\text{Fe}_\odot$  or  $(\text{Fe}/\text{Fe}_\odot)^{0.7}$ , the predicted 7/6 ratio is

$${}^7\text{Li}/{}^6\text{Li} = R_{76} + \frac{(1 + R_{76})a}{bx} \quad (1)$$

At present, detections of  ${}^6\text{Li}$  are claimed for three metal-poor stars (Smith, Lambert, & Nissen 1993, 1998, Hobbs, & Thorburn 1991, 1997, Hobbs, Thorburn, & Rebull 1999, Nissen *et al.* 1999, Nissen *et al.* 2000) two of which are included in the RNB sample. In Figure 5 we compare the observed 6/7 ratios with those predicted by RNB evolution for  $1.5 \lesssim R_{76} \lesssim 1.6$ . While the post-BBN evolution suggested by RNB may account for the observed 6/7 ratio in one (possibly two) stars, it is clear that it is too rapid to satisfy all the observational data.

Of course, if we are correct that some depletion via rotational mixing can have occurred in one or more of these stars, it may be that the observed 6/7 ratios are not representative of the prestellar values. As an illustration, we show by the open circles in Figure 5 the predictions for our standard (*i.e.*, no rotational mixing or gravitational settling) model depletion. We emphasize though that these “predicted” data points should not be compared to the evolution curves which have been derived on the assumption of no depletion. Nonetheless, it is clear that no simple model for post-BBN lithium production can account for all three data points in the absence of some  ${}^6\text{Li}$  depletion. We note that the two stars in the RNB sample (HD 84937 and BD +26 3578) have lithium abundances slightly above the (undepleted) plateau (2.17 and 2.15 respectively); this may indicate that they are detectable because they are a bit underdepleted within the rotational mixing context.

#### 4. Observational Data

In the preceding sections we have compared our results with the RNB data sample reaching qualitatively similar conclusions to those drawn from earlier data sets, in particular from the large T94 sample that we used in PWSN. However, there are some observational differences, and it is important to identify how and why the various observational data sets differ. RNB obtained lithium observations for 23 halo stars; one star (G186-26) had only an upper limit and was excluded from their dispersion analysis. The RNB sample of stars were chosen in a narrow  $T_{\text{eff}}$  range with a low metal abundance. 18 of the 22 remaining stars were also studied in T94, a sample designed with similar goals. There were also 18 stars in common with the earlier Ryan *et al.* (1996) data set and 10 stars in common with the

Spite & Spite (1993) sample (Spite *et al.* (1996), Spite & Spite (1982), Spite, Maillard, & Spite (1984); hereafter SS). Because the Ryan *et al.* (1996) sample is dominated by the large number of stars from the T94 sample, there are really only two independent, primary samples which may be compared with RNB: T94 and the SS sample.

## 4.1. Comparison with Other Data Sets

### 4.1.1. Comparison with T94: The Origin of Differences in Zero-point and Dispersion

The conclusions drawn by RNB and T94 are markedly different despite the significant overlap in the two samples and their similar goals and design. We therefore begin by examining the ingredients that could be responsible for this difference, namely 1) the statistics of the subset of the T94 data set studied by RNB, relative to the statistics of the entire T94 data set; 2) the choice of effective temperature scale; 3) the equivalent width measurements and; 4) the model atmospheres used to relate equivalent width and effective temperature to abundance.

The raw dispersion measured by RNB for their sample of 22 stars (0.052 dex) is very similar to the raw dispersion for the subset of their 18 stars in common with T94 (0.054 dex), suggesting that the stars not in common do not strongly influence the overall result. The raw dispersion for the full T94 sample was 0.13 dex, similar to the dispersion of 0.12 dex that would be inferred for the subset of 18 stars from the T94 data. Therefore, the RNB data set appears to be a fair subsample of the T94 data set. This is not surprising since both were chosen using similar kinematic, metal abundance, and effective temperature criteria. However, the average abundances for the stars in common derived by RNB and by T94 differ significantly, 2.11 and 2.29 respectively.

In subsequent steps we examined the impact of changes in the temperature scale and equivalent widths. The  $T_{\text{eff}}$  scale chosen by RNB is different (and on average cooler) than that used by T94. To estimate the importance of this effect, we compared the temperatures used by RNB and T94. We used the RNB slope of 0.065 dex per 100K to infer the lithium abundances that T94 would have obtained using the RNB temperature scale. If the different temperatures adopted by T94 and RNB were responsible for the different conclusions about the sample dispersion we would expect a large decrease in the sample dispersion by performing this operation while retaining the T94 equivalent widths and model atmospheres. Adopting the RNB temperatures reduces the average abundance inferred using the T94 equivalent widths and atmosphere model only from 2.29 to 2.25, while actually slightly increasing the dispersion that would have been inferred from the T94 data relative to the

T94  $T_{\text{eff}}$  scale. The abundances that would have been inferred from the T94 equivalent widths and model atmospheres with the RNB  $T_{\text{eff}}$  scale are given in Table 2 (see section 2). We conclude that while the choice of temperature scale does influence the abundance zero-point, the different temperature scales do not explain the difference in the dispersion of the samples. We illustrate this in Figure 6, where the RNB abundances are compared with the T94 abundances for stars in common shifted to the same  $T_{\text{eff}}$  scale. The intrinsic scatter is clearly larger for the T94 equivalent widths, even accounting for the larger formal equivalent width error bars.

We also derived the abundances that T94 would have obtained had both the lithium equivalent widths and temperatures of RNB been used instead of the EW and  $T_{\text{eff}}$  as adopted by T94. The sole remaining difference after this has been done is the choice of model atmospheres relating equivalent width, temperature, and abundance. For this test we used the linear curve of growth approximation; e.g. the corrected  $[\text{Li}/\text{H}] = [\text{Li}/\text{H}](\text{T94}) + \log(\text{EW RNB}/\text{EW T94})$ . Changing the equivalent widths (along with  $T_{\text{eff}}$ ) leads to a large decrease in the dispersion, from 0.13 dex to 0.07 dex; furthermore, the average inferred abundance decreases to 2.22. The average difference between the equivalent width measurements of RNB and T94 is 1.9 mÅ (in the sense that T94 is systematically higher), so there is both a zero-point shift and a difference in the range of equivalent widths at fixed  $T_{\text{eff}}$  in the RNB sample relative to the T94 sample.

We attribute the remaining zero-point shift to one of two effects. The linear curve of growth assumption that we have employed could introduce some errors; T94 and RNB also used different model atmospheres to relate abundance to equivalent width. Ryan *et al.* (2000) estimate the systematic differences arising from the different model atmospheres to be at the  $\sim 0.08$  dex level, which can account for all but a small (0.03 dex) difference in the mean abundance. We therefore conclude that the reason for the significantly different RNB dispersion estimates from those of T94 are due to differences in the underlying basic equivalent width data and not by the choice of  $T_{\text{eff}}$ , the sample properties, or the model atmospheres. In contrast, the difference in the lithium abundance zero-point can be attributed to a combination of a different  $T_{\text{eff}}$  scale, systematically lower RNB equivalent widths relative to T94, and the choice of different model atmospheres. This leads to a large overall difference between the mean abundances derived for stars in common, corresponding to a change in the inferred primordial lithium abundance comparable to the lower end of the range of stellar depletion presented in PWSN.

There is an average zero-point offset of 2.5 mÅ in the RNB sample relative to the SS data set; a similar effect compared was discussed in Ryan *et al.* (1996). The overall morphology is similar to that between T94 and RNB: 2 out of 10 points differ by more than  $2\sigma$  even

when the zero-point offset is taken into account. For completeness, we note that there is also a zero-point offset of 0.8 mA relative to the Ryan *et al.* (1996) analysis; as mentioned above, because this sample is heavily weighted by the T94 sample we did not perform a separate comparison of the Ryan *et al.* (1996) and RNB samples. We therefore conclude that zero-point differences in equivalent width measurements appear to be significant, and by themselves they contribute an uncertainty of order 10 % to the absolute abundances.

#### 4.2. Interpretation of the Differences

Even before reducing the dispersion by appealing to chemical evolution trends, the RNB sample has a smaller dispersion than does the T94 sample. RNB attributed the differences between their data and that of T94 to an underestimate of the errors in the T94 data. In particular, T94 did not correct for scattered light and sky subtraction. RNB note that this could increase the formal errors of individual data points in the T94 sample by a factor up to 1.7. In this case, one would not expect a gaussian distribution of the differences in equivalent widths, since the T94 stars with the largest relative errors from these effects would be affected more than those where the quoted T94 error estimates are accurate. There is an independent test of this hypothesis: we can compare the results of SS with those of T94. If the most discrepant points are due to larger than expected errors in the T94 measurements, then there is no reason to expect the SS sample to have encountered the same problems.

In Figure 7 we compare equivalent width measurements for stars from different sources (RNB, T94, SS). The three left-hand panels compare the eight stars with measurements from all three sources; the right panels compare RNB with the stars in common with the T94 and SS data sets, respectively. Although the overlap among the samples is small (eight stars), we see no direct evidence that the T94 data is in conflict with the two other data sets; similarly, Ryan *et al.* (1996) found a good correlation between the SS data and the T94 data once a zero-point offset was taken into account.

In light of the ambiguous results above, it is worth returning to the question of what degree of stellar depletion is consistent with the T94 data. Because the RNB  $T_{\text{eff}}$  errors are significantly smaller than the T94 errors, the average error using the T94 equivalent widths is reduced to 0.06 dex. This provides a smaller but more precise sample than the one used in PWSN.

Adopting the T94 equivalent widths instead of the RNB equivalent widths produces a significantly different cumulative distribution. We compare the observed distribution with theoretical simulations convolved with a  $\sigma = 0.06$  dex gaussian in Figure 8. The s0.3 case

with 0.32 dex depletion is now the best fit, while the 0.18 and 0.5 dex depletion cases are only marginally consistent. We include this to emphasize that the differences between the observational data sets needs to be reconciled in order to set more precise bounds on stellar depletion.

In conclusion, we find that the large difference between the results of RNB and T94 in their dispersion analyses can be traced directly to equivalent width measurements. The overall deviations exceed those predicted from the quoted errors. There are significant zero-point offsets, and external comparison with a small overlap sample from SS does not clearly identify a problem with the T94 values. We therefore caution that further observational work is likely needed to uncover the origin of the differences, particularly since the overall conclusions depend sensitively on the presence or absence of a small number of outliers.

## 5. Discussion

Knowledge of the primordial lithium abundance sets interesting constraints on Big Bang Nucleosynthesis. However, the determination of the primordial lithium abundance relies both on observational data as well as on the model for stellar depletion. The most recent  ${}^7\text{Li}$  abundance data sets exhibit a core with little internal scatter and a small number of outliers; these properties have been used to argue that there is little, if any, room for any stellar depletion. We have analyzed the RNB data set, and find that with or without accounting for a trend with metal abundance the data is consistent with mild stellar depletion; the best fit depletion is in the range of 0.1 –– 0.2 dex . Theoretical models with rotational mixing depletion this low predict a core with small scatter, since the large majority of young stars have low, and similar, rotation rates. Therefore, the number of outliers is a stronger test of the presence or absence of dispersion from rotational mixing. Either the no depletion case or models with lithium as depleted as 0.5 dex are unlikely based on both KS tests and the predicted number of overdepleted outliers as compared with the observed number. Our results differ from those of RNB because they detrended the data in the  $\log(\text{Li})$  ––  $\text{Log}(\text{Fe})$  plane rather than in the linear  $\text{Li}$  –– linear  $\text{Fe}$  plane which is more appropriate when testing for the presence of post-BBN  ${}^7\text{Li}$  production. Similar conclusions can be derived from the observed ratio of  ${}^6\text{Li}$  to  ${}^7\text{Li}$ .

We have also compared the T94 and RNB data sets, and find that the different conclusions that the two papers drew about the dispersion in lithium among halo stars can be traced directly to differences in equivalent width. If the T94 equivalent widths are used instead of the RNB equivalent widths, a stellar depletion factor of 0.3 dex is inferred. We find no compelling evidence of problems in the T94 data by comparing both it and RNB

with an (admittedly small) set of stars in common with other studies. This indicates that there is further work to do on the observational front before making sweeping claims with implications for cosmology. Systematic observational errors from the temperature scale (0.05 dex), choice of model atmospheres (0.08 dex), and equivalent width zero-point errors (0.05 dex) alone yield an uncertainty of 0.11 dex in the observed  ${}^7\text{Li}$  abundance before considering stellar depletion — an error of similar magnitude to the theoretical uncertainties. In the last two sections we discuss the issues and uncertainties involved in the stellar modelling and the implications for BBN.

### 5.1. Stellar Physics Models

Further improvements are also desirable in the theoretical modelling of mixing and diffusion processes in the envelopes of low mass stars. These fall into the general categories of improved stellar physics on the one hand and better knowledge of the distribution of initial conditions and the angular momentum loss law on the other hand.

In Population I stars we have extensive empirical data on the distribution of rotation rates as a function of mass and age. We can only observe very metal poor stars when they are old, and therefore must extrapolate the behavior of Population I stars into a different metallicity regime. The best prospect for constraining the theory is in observations of young clusters of intermediate metallicity; this will permit a direct test of the distribution of rotation rates and their time evolution. If the fraction of rapid rotators is different from that present in Population I open clusters, the predicted number of outliers would be affected. More efficient angular momentum loss in metal-poor stars could also reduce the predicted number of overdepleted stars for a given absolute depletion.

On the stellar physics side, the important uncertainties are internal angular momentum transport and the interaction of gravitational settling and rotational mixing. Helioseismic data indicates that the solar internal rotation is independent of depth in the radiative core down to 0.2 solar radii (e.g. Chaplin *et al.* (1999)); the situation in deeper layers is less certain (compare Chaplin *et al.* (1999) with Gavryuseva, Gavryusev, & di Mauro (2000)). The spindown of young open cluster stars, however, is not consistent with uniform rotation enforced on a very short timescale (Krishnamurthi *et al.* (1997)). This combination implies that the timescale for effective angular momentum coupling between the surface and interior is intermediate between the ages of the young open clusters (50-100 Myr) and the Sun (4.57 Gyr.) We are currently evaluating models in the limiting case of uniform rotation at all times to infer the impact on the predicted depletion. The general sense would be to reduce lithium depletion in models with shallower convection zones (because the diffusion coefficients are

larger if the core rotates more rapidly than the surface.) Therefore the predicted degree of depletion in halo stars for a given solar calibration will be reduced. However, a range of stellar depletion factors for a range in solar initial conditions will still be possible; the net effect will be to make the observed halo star depletion consistent with less extreme values of the solar initial conditions.

Finally, gravitational settling and microscopic diffusion could affect surface lithium abundances. The gravitational settling of helium will produce a mean molecular weight gradient below the surface convection zone; composition gradients could reduce the effect of mixing (see Zahn (1992) for a discussion.) If rotational mixing was simply suppressed, however, models with gravitational settling predict a decrease in halo star surface lithium with increased effective temperature which is not observed (Chaboyer *et al.* (1992)). Vauclair (1999) has raised the possibility of a nonlinear interaction that results in the suppression of both mixing and diffusion. This is an interesting possibility that should be investigated. There are, however, some factors that make a complete cancellation unlikely in our view.

First, the physical conditions in Population I stars with temperatures similar to the plateau stars are not very different from the halo star conditions. We observe strong depletion and dispersion in M67 stars with temperatures around 6200K, which suggests that mixing is not inhibited in solar abundance stars where the timescale for gravitational settling is similar to the halo star case. In addition, Chaboyer, Demarque, & Pinsonneault (1995) investigated the interaction of gravitational settling and mixing for an earlier generation of models. They found that the time and mass dependence of lithium depletion was difficult to reconcile with a strong suppression of mixing by settling. It is important to test the interaction of these physical processes against Population I data. In addition to the lithium question, such models must address the apparent absence of a gravitational settling signature in the turnoff region of globular clusters (Chaboyer *et al.* (1992); Bergbush & Vandenberg (2001)).

## 5.2. Implications for BBN

Uncertainties in lithium equivalent width measurements, temperature scales, and model atmospheres introduce a *systematic* error in the determination of lithium abundances (on the log scale) which we estimate as  $\pm 0.1$  dex, in agreement with Ryan *et al.* (2000)’s detailed analysis of the error budget. Reflecting this uncertainty, the level of the Spite plateau, before accounting for depletion by rotational mixing or for post-BBN lithium production, has been variously estimated as 2.1 (RNB), 2.2 (Bonifacio & Molaro (1997), Bonifacio, Molaro, & Pasquini (1997)), and 2.3 (T94). We adopt  $2.2 \pm 0.1$  for our baseline estimate. We have found that the residual dispersion in the RNB data is well accounted for in a model

of stellar depletion induced by rotational mixing, even without account of the additional dispersion that might be due to a real spread in halo star abundances due to post-BBN lithium production. Our best estimate of the overall depletion factor consistent with the RNB data set is 0.13 dex, with a 95% range extending from 0.0 to 0.5 dex. Similarly, using the T94 equivalent widths we find an overall best-fit depletion of 0.32 dex. For all of the reasons given above, we believe that modest stellar depletion factors are consistent with the data. At the same time, the sample size is small and these conclusions are subject to Poisson noise. Given that the expected fraction of overdepleted stars from rotational mixing is of order 15%, even adding or subtracting a single star from the sample can have a significant impact on the inferred depletion. With this in mind, we adopt an overall depletion factor of  $0.2 \pm 0.1$  dex and, adding this correction to our baseline estimate (and combining these systematic uncertainties linearly), we derive a primordial lithium abundance of  $2.4 \pm 0.2$ .

Having established an observed halo lithium abundance of  $2.2 \pm 0.1$  and our best estimate of the primordial lithium abundance of  $2.4 \pm 0.2$  (based on both the observed abundance and a theoretical determination of the depletion required by the dispersion in the observed abundance), we can now compare to the primordial lithium abundance predicted by standard BBN. As previously mentioned, in standard BBN the predicted abundances of the light nuclides is a function of one parameter, the baryon-to-photon ratio  $\eta$ . Within the errors introduced by uncertainties in the weak and nuclear cross sections, the predicted abundances of D,  $^3\text{He}$ ,  $^4\text{He}$ , and  $^7\text{Li}$  follow from a determination of  $\eta$ . The predicted abundance of deuterium depends most strongly on  $\eta$  and, using the observed D/H as measured in high-redshift QSO absorption line systems (Burles & Tytler 1998a,b; O’Meara *et al.* 2000), it can be used as a “baryometer”:  $\eta_{10} \equiv 10^{10}(n_B/n_\gamma) = 5.6 \pm 0.5$  ( $1\sigma$ ). The predicted lithium abundance corresponding to this range of baryon densities is  $[\text{Li}]_P = 2.3$  to  $2.8$  ( $(\text{Li}/\text{H})_P = 2 - 6 \times 10^{-10}$ ), inconsistent with the Ryan *et al.* 2000 halo star lithium abundance, but in good agreement with our estimate for the primordial lithium abundance. Our range of predicted Li/H is based on the OSW 2000  $1\sigma$  range (Olive, Steigman, & Walker (2000) and references therein), which is broader than, but consistent with that of Burles, Nollett, & Turner (2000), which for the same  $\eta$  range predicts  $[\text{Li}]_P = 2.4$  to  $2.7$ . The NACRE collaboration’s (Angulo *et al.* (1999)) compilation yields a similar but slightly lower range than that of Burles, Nollett, & Turner (2000). We note that recent deuterium observations (D’Odorico, Dessauges-Zavadsky, & Molaro (2001), Pettini & Bowen (2001)) suggest that the damped Lyman  $\alpha$  systems may have systematically lower D/H than the Lyman limit systems. The lower D/H would correspond to an even higher BBN Li/H, further exacerbating the disagreement with the Ryan *et al.* 2000 lithium abundance, and even pushing the upper envelope of our model-dependent estimate of the primordial abundance. The situation is summarized in Figure 9, where we show as a band, the standard BBN-predicted abundance

of Li/H as a function of the BBN-predicted D/H. The “data point” is for the O’Meara *et al.* 2000 deuterium abundance and the Ryan *et al.* 2000 lithium value. The horizontal band corresponds to our estimate of the depletion-corrected primordial lithium abundance. The Ryan *et al.* 2000 inferred primordial lithium abundance is too small, by a factor or two or more, to be consistent with the deuterium-based BBN prediction. In contrast, there is excellent overlap between our depletion-corrected estimate ( $[\text{Li}]_P = 2.4 \pm 0.2$ ) and the deuterium-constrained BBN prediction. Consistency with BBN *requires* that lithium has been depleted in the metal-poor halo stars of the Spite plateau by an amount consistent with that predicted by our models of rotational mixing induced stellar depletion.

M.P. wishes to acknowledge support from the NASA Astrophysics Theory Program (grant NAG5-7150.) The work of G.S. and T.P.W. is supported by DOE grant DE-FG02-91ER40690.

## REFERENCES

- Angulo, C., *et al.* 1999, Nucl. Phys. A., 656, 3 (NACRE)
- Balachandran, S. 1995, ApJ, 446, 203
- Beers, T.C., Preston, G.W., & Shectman, S.A. 1992, AJ, 103, 1987
- Bergbush, P.A. & Vandenberg, D.A. 2001, ApJ, in press (astro-ph/0202480)
- Boesgaard, A.M., King, J.R., Deliyannis, C.P., & Vogt, S.S. 1999, AJ, 117, 492
- Bonifacio, P. & Molaro, P. 1997, MNRAS, 285, 847
- Bonifacio, P., Molaro, P. & Pasquini, L. 1997, MNRAS, 292, L1
- Burles, S., Nollett, K.M., & Turner, M.S. 2000, ApJ, in press, astro-ph/0010171
- Carney, B.W., Latham, D.W., Laird, J.B., & Aguilar, L.A. 1994, AJ, 107, 2240
- Chaboyer, B.C. *et al.* 1992, ApJ, 388, 372
- Chaboyer, B.C., Demarque, P., & Pinsonneault, M.H. 1995, ApJ, 441, 876
- Chaplin, W.J. *et al.* 1999, MNRAS, 308, 405
- Deliyannis, C.P., Demarque, P., & Kawaler, S.D. 1990, ApJS, 73, 21

- D’Odorico, S., Dessauges-Zavadsky, M., & Molaro, P. 2001, A&A in press, astro-ph/0102162
- Fulbright, J.P. & Kraft, R.P. 1999, AJ, 118, 527
- Gavryuseva, E.A., Gavryusev, V.G., & di Mauro, M.P. 2000, Ast. Lett., 26, 261
- Hobbs, L.M. & Thorburn, J.A. 1991, ApJ 375, 116; *ibid* 1997, 491, 772
- Hobbs, L.M., Thorburn, J.A., & Rebull, L.M. 1999, ApJ, 523, 797
- Israelian, G., Garcia-Lopez, R.J., Rebolo, R. 1998, ApJ, 507, 805
- Jones, B.F., Fischer, D., & Soderblom, D. 1999, AJ, 117, 330
- King, J.R. 2000, AJ, 120, 1056
- Kneller, J.P., Phillips, J.R., & Walker, T.P. 2000, submitted to ApJ, astro-ph/0008073
- Krishnamurthi, A., Pinsonneault, M.H., Barnes, S., & Sofia, S. 1997, ApJ, 480, 303
- Nissen, P.E., Asplund, M., Hill, V., & D’Odorico, S. 2000, A&A, 357 L49
- Nissen, P.E., Lambert, D.L., Primas, F., & Smith, V.V. 1999, A&A, 348, 211
- Olive, K.A., Steigman, G., & Walker, T.P. 2000, *Phys. Rep.*, 333-334, 389
- Pettini, M. & Bowen, D.V. 2001, submitted to ApJ, astro-ph/0104474
- Pinsonneault, M.H., Deliyannis, C.P., & Demarque, P. 1992, ApJS, 78, 181
- Pinsonneault, M.H. 1997, ARA&A, 35, 557
- Pinsonneault, M.H., Walker, T.P., Steigman, G., & Narayanan, V.K. 1999, ApJ, 527, 180
- Reeves, H., Fowler, W.A., & Hoyle, F. 1970, Nature, 226, 727
- Ryan, S.G., Beers, T.C., Deliyannis, C.P., and Thorburn, J.A. 1996, ApJ, 458, 543
- Ryan, S.G., Beers, T.C., Kajino, T., & Rosolankova, K. 2001, ApJ, 547, 231
- Ryan, S.G., Beers, T.C., Olive, K.A., Fields, B.D., & Norris, J. E. 2000, ApJ, 530, L57
- Ryan, S.G. & Norris, J.E. 1991, AJ, 101, 1865
- Ryan, S.G., Norris, J.E., & Bessel, M.S. 1991, AJ, 102, 303
- Ryan, S.G., Norris, J.E., & Beers, T.C. 1999, ApJ, 523, 654

- Smith, V.V., Lambert, D.L., & Nissen, P.E. 1993, *ApJ*, 408, 262; *ibid* 1998, 506, 405
- Spite, M., Francois, P., Nissen, P.E., & Spite, F. 1996 *A&A*, 307, 172
- Spite, M., Maillard, J. P., & Spite, F. 1984, *A&A*, 141, 56
- Spite, F. & Spite, M. 1982, *A&A*, 115, 357
- Spite, F. & Spite, M. 1993, *A&A*, 279, L9
- Steigman, G. & Walker, T.P. 1992, *ApJ*, 385, L13
- Suzuki, K.S., Yoshii, Y., & Beers, T. C. 2001, *ApJ*, 540, 99
- Thorburn, J.A. 1994, *ApJ*, 421, 318
- Vauclair, S. 1999, *A&A*, 351, 973
- Zahn, J.-P. 1992, *A&A*, 265, 115

Fig. 1.— The cumulative observed distribution of RNB is compared with the distributions expected from Gaussian errors with  $\sigma = 0.035$  dex (short dashed line) and the s0 (medium-dashed line), s0.3 (dot-dash line), and s1 (long-dashed line) distributions from PWSN convolved with the same error. The zero-point of the theoretical distributions is set by anchoring the median depletion factors of 0.18 dex, 0.32 dex, and 0.50 dex respectively at the sample median of 2.11.

Fig. 2.— Chemical evolution fits to the RNB data set using the RNB literature metal abundances (top panel) and the RNB low resolution metal abundances (bottom panel) in the linear Li - linear Fe plane. The solid line includes all stars; the dashed lines excludes the stars identified as outliers in RNB.

Fig. 3.— Chemical evolution fits to the RNB data set using the RNB literature metal abundances (top panel) and the RNB low resolution metal abundances (bottom panel) under the assumption of strong oxygen enhancement in metal poor stars. We mapped Fe onto Z as described in the text and performed a least-squares fit in the linear Li - linear Z plane. The solid line includes all stars; the dashed line excludes the stars identified as outliers in RNB.

Fig. 4.— The RNB data presented here has been corrected to zero metal abundance using the LL model slope including all stars. The cumulative observed distribution of RNB corrected for chemical evolution is compared with the distributions expected from Gaussian errors with  $\sigma = 0.04$  dex (short dashed line) and the s0 (medium-dashed line), s0.3 (dot-dash line), and s1 (long-dashed line) distributions from PWSN. The zero-point of the theoretical distributions is set by anchoring the median depletion factors of 0.18 dex, 0.32 dex, and 0.50 dex respectively at the sample median of 2.07.

Fig. 5.— The measurements of  ${}^6\text{Li}$  to  ${}^7\text{Li}$  (filled circles) are compared with the predictions of the different chemical evolution models; the solid lines correspond to the range of uncertainties for the high-slope cases and the dashed lines correspond to the range of uncertainties for the low slope cases. The top panel uses the linear Li - linear Fe fits and the bottom panel estimates the effect of strong oxygen enhancement in the most metal-poor stars in the same fashion as Figure 3. See text for data sources; the open circles include a classical model  ${}^6\text{Li}$  depletion factor of 0.2 dex for the two more metal-rich detections.

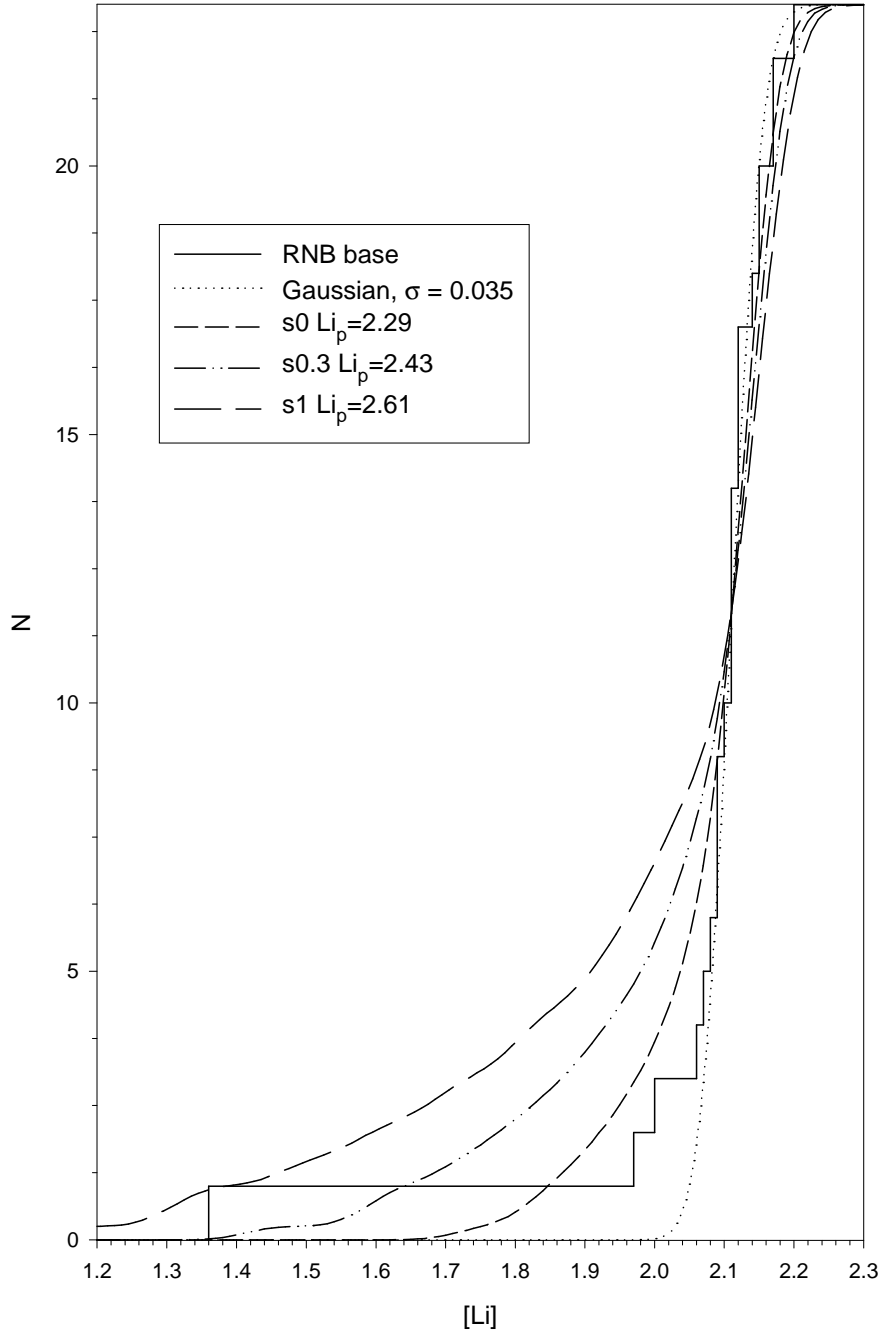
Fig. 6.— The RNB data set (top panel) is compared with the T94 data set under three different assumptions. The published T94 data for stars in common is presented in the second panel. The third panel shows the effect of replacing the T94  $T_{\text{eff}}$  values with those from RNB. The bottom panel shows the effect of replacing both the temperatures and equivalent width measurements of T94 with the RNB values under the assumption of a linear curve of growth.

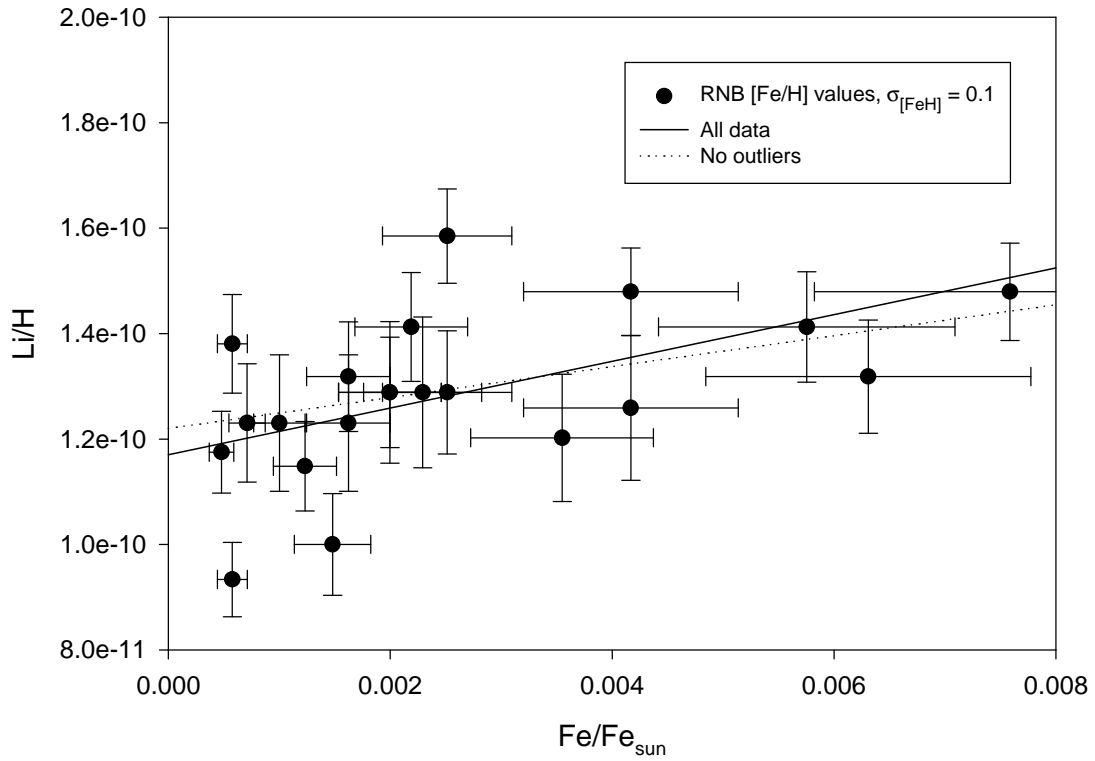
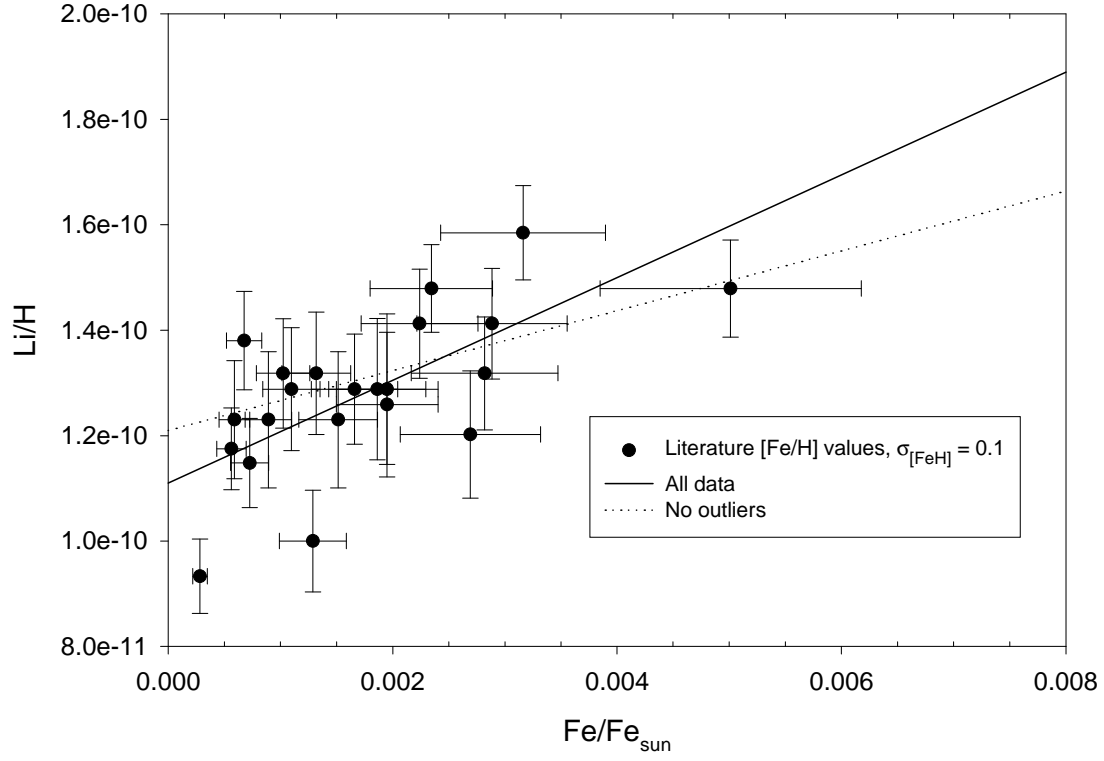
Fig. 7.— Equivalent width measurements from RNB, T94, and SS are compared in this figure. The left three panels include stars in common to all three sets. RNB data are compared to SS data in the top left panel; RNB compared to T94 data in the middle left panel; and SS compared to T94 in the bottom left panel. The two right panels compare the RNB data with the full overlap sample of SS (top right) and T94 (bottom right.)

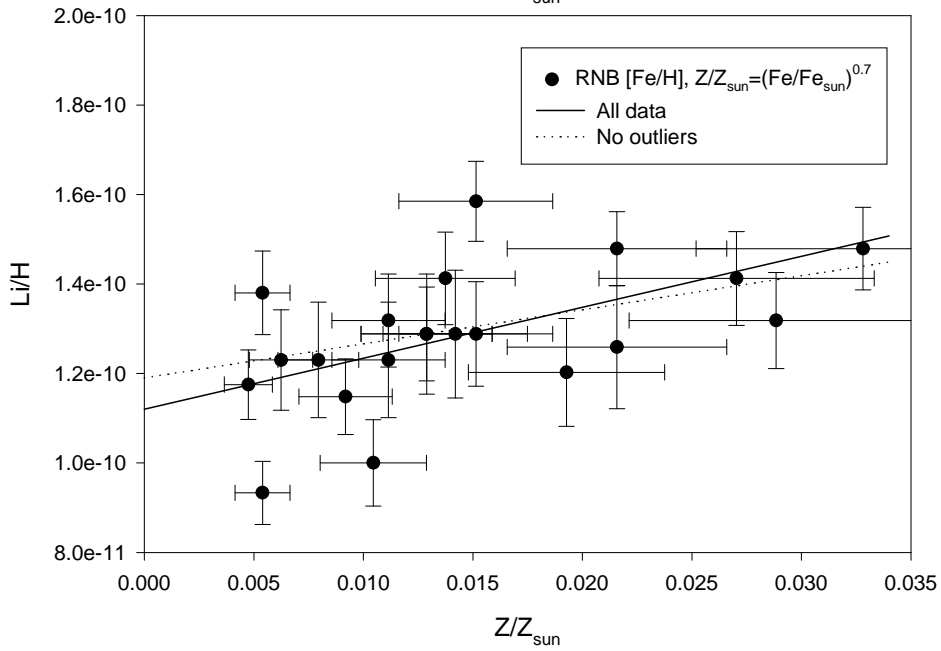
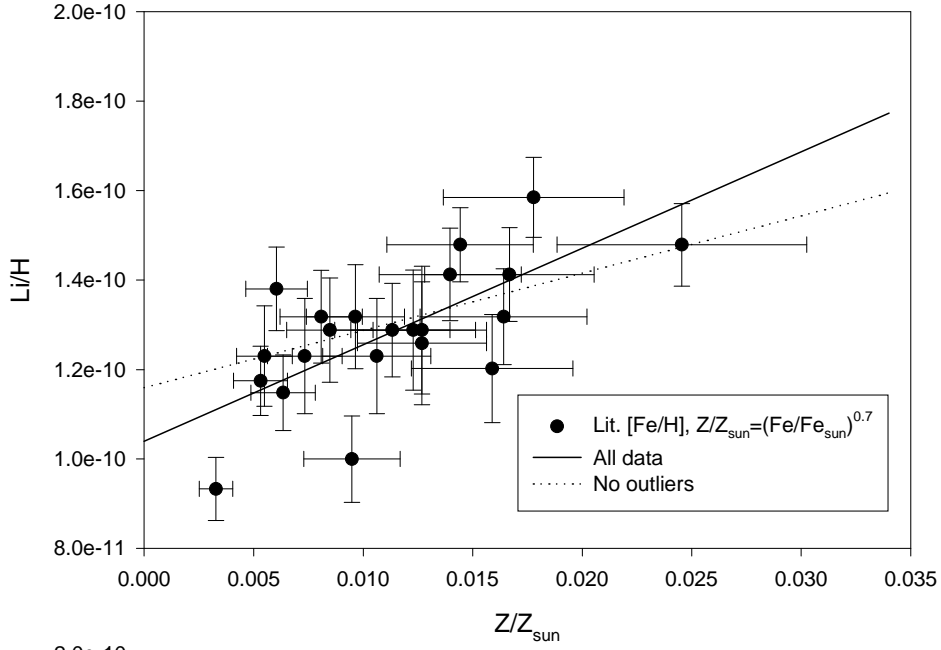
Fig. 8.— The cumulative observed distribution of the RNB sample using the T94 model atmospheres and equivalent widths is compared with the distributions expected from Gaussian errors with  $\sigma = 0.06$  dex (short dashed line) and the s0 (medium-dashed line), s0.3 (dot-dash line), and s1 (long-dashed line) distributions from PWSN convolved with the same error. The zero-point of the theoretical distributions is set by anchoring the median depletion factors

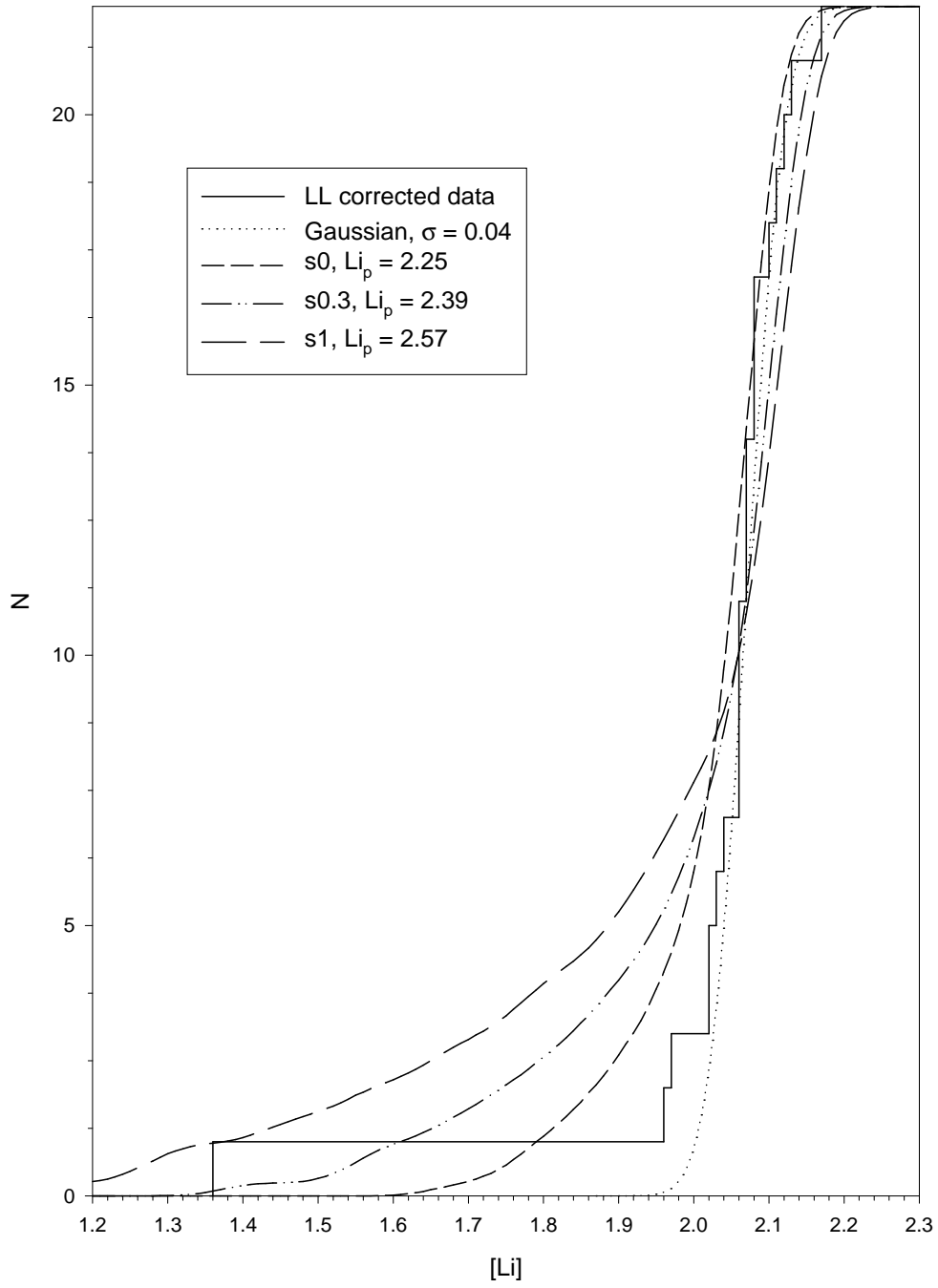
of 0.18 dex, 0.32 dex, and 0.50 dex respectively at the sample median of 2.25.

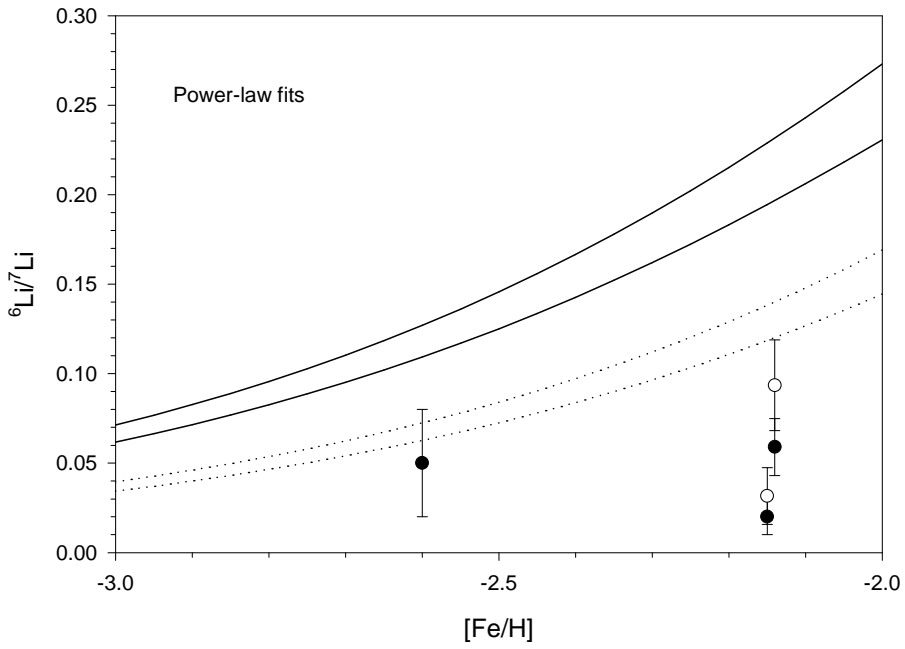
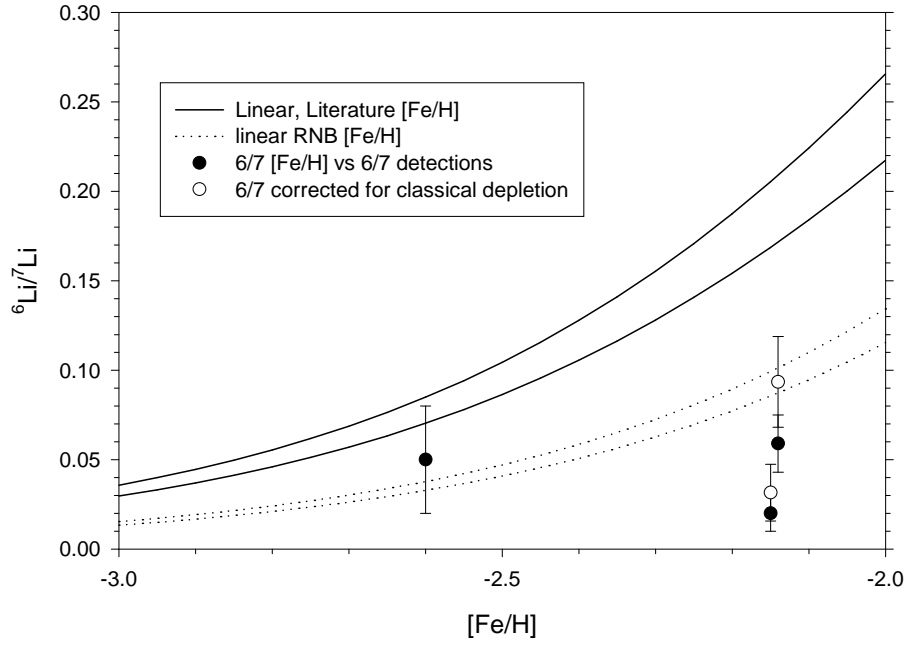
Fig. 9.— The solid curves show the  $\pm 1\sigma$  range for the BBN-predicted relation between primordial lithium and primordial deuterium. The point with error bars is the O’Meara *et al.* deuterium value and the Ryan *et al.* (2000) lithium estimate. The horizontal band is our depletion-corrected lithium estimate, and the vertical band indicates the observed range for deuterium.

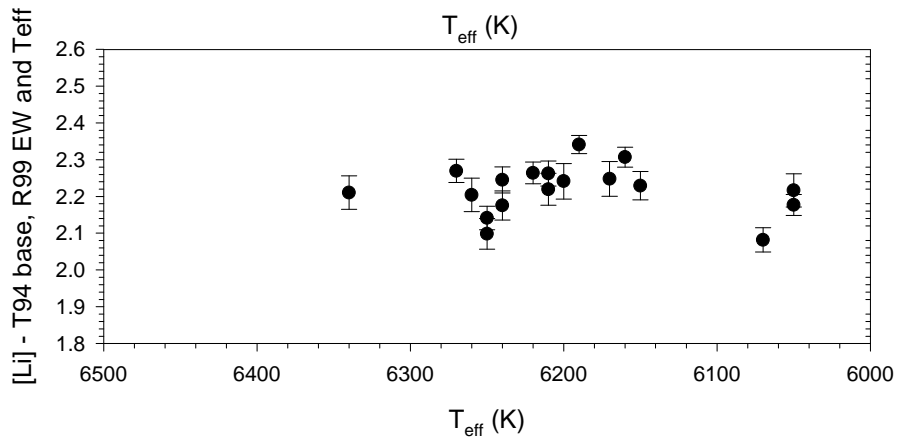
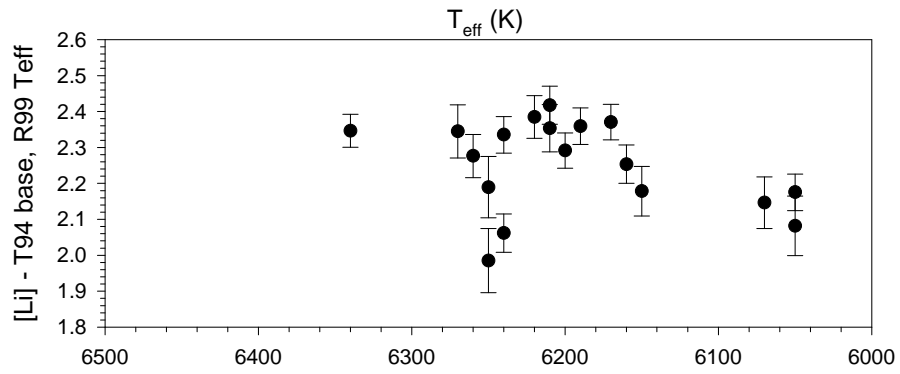
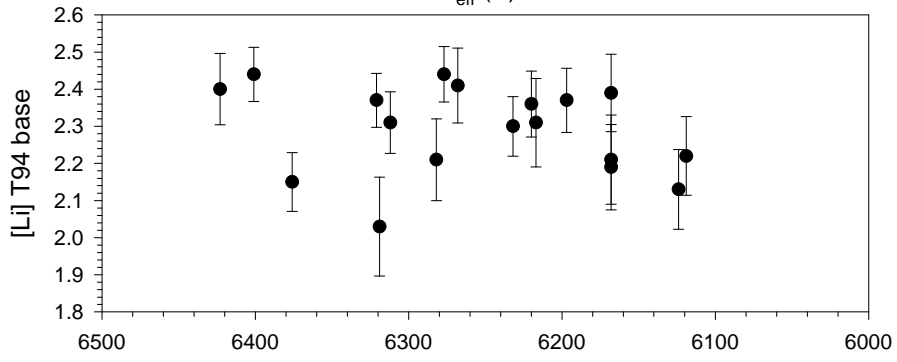
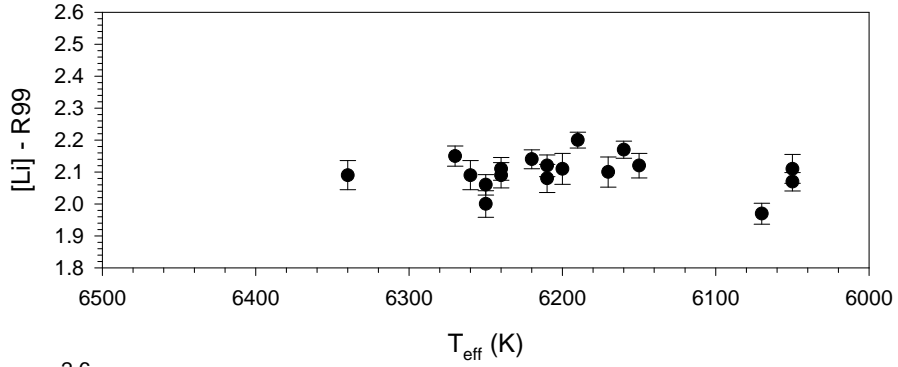


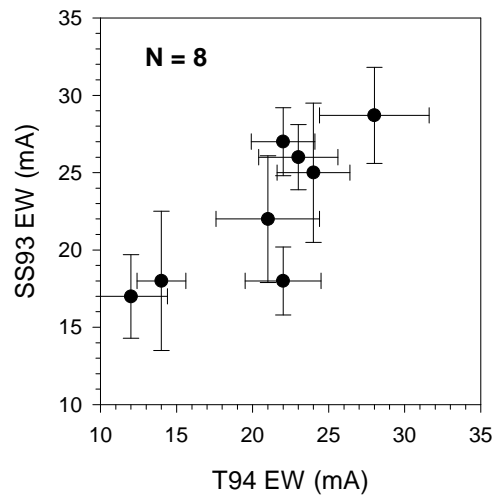
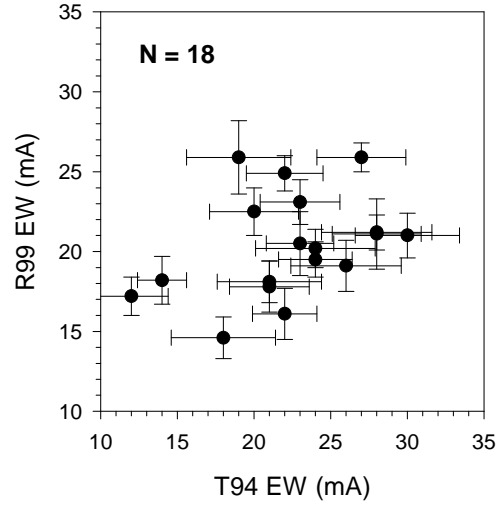
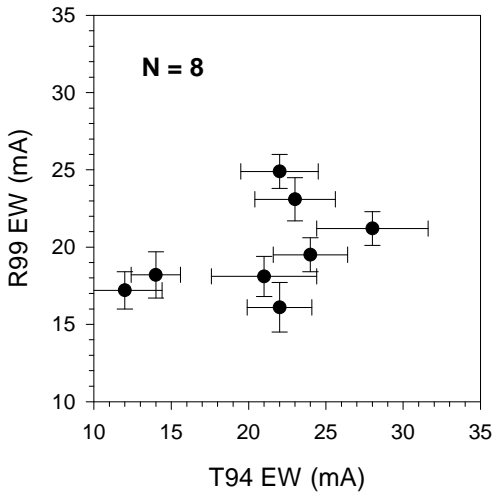
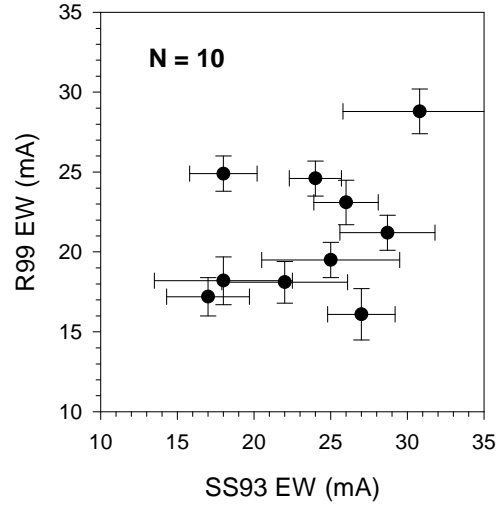
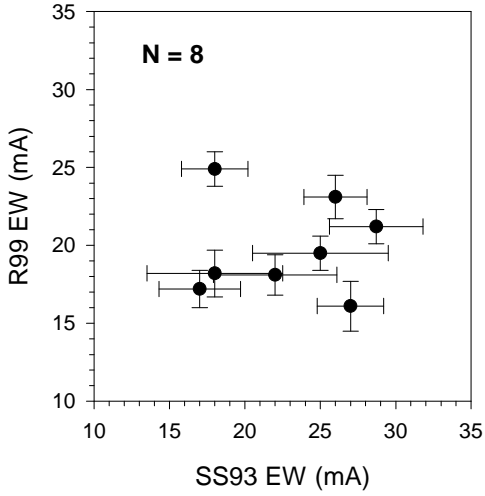


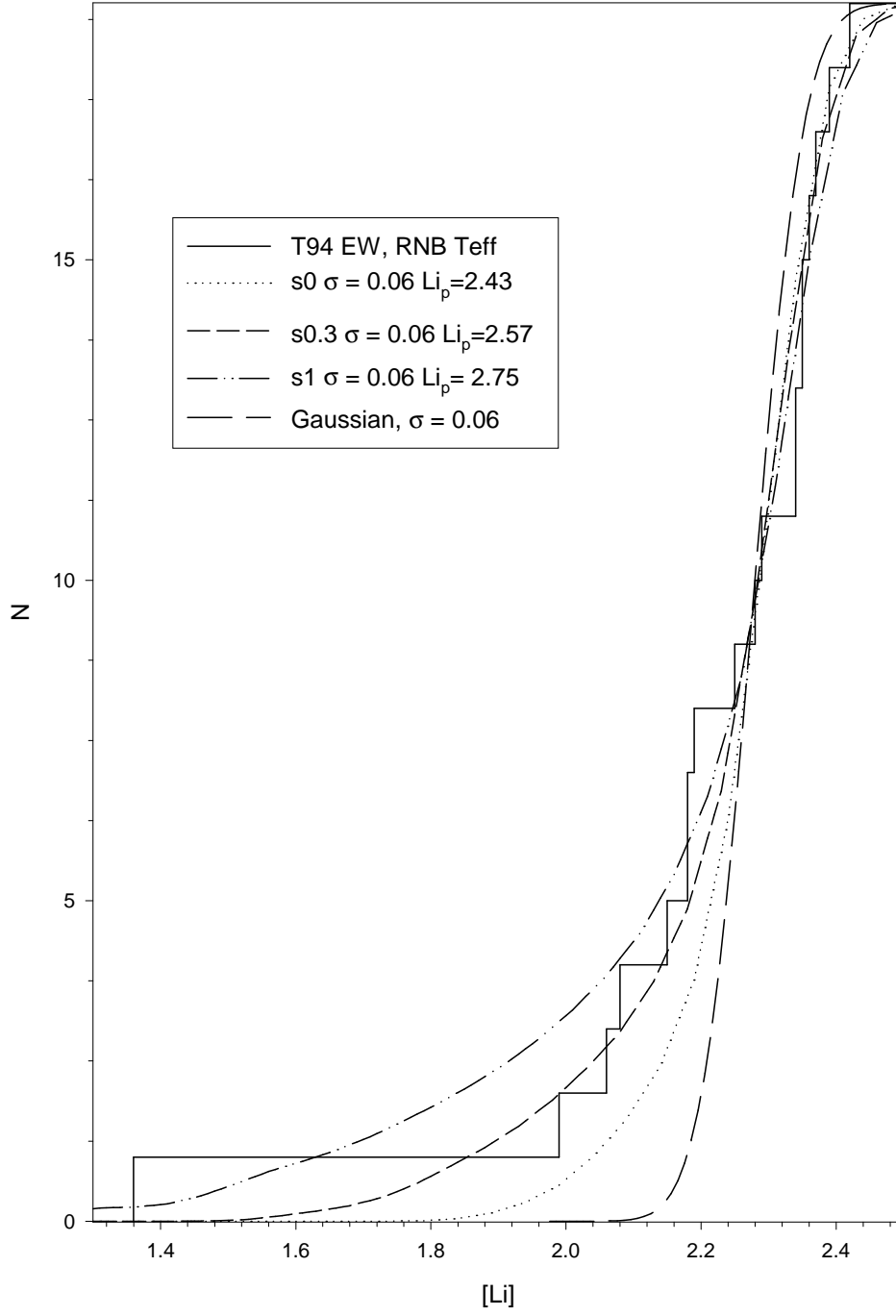












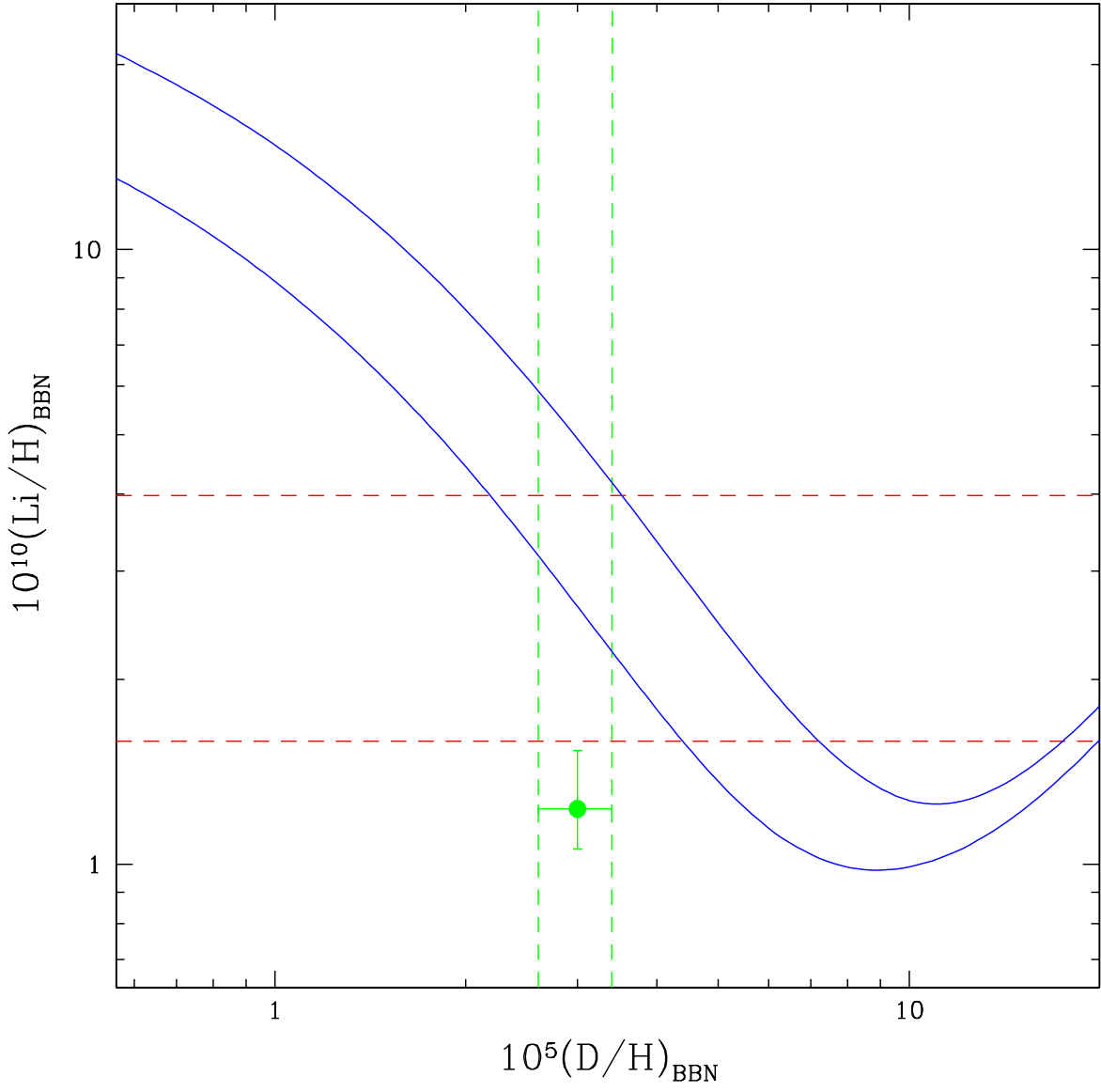


Table 1. Outlier Tests, No Evolution

| Case     | $\log(Li/Li_o)$ | Probability<br>< 2.06 | Probability<br>< 2.01 |
|----------|-----------------|-----------------------|-----------------------|
| Gaussian | 0.00            | 0.114 (1.0)           | 0.00005 (0.02)        |
| s0       | -0.18           | 0.45 (3.7)            | 0.11 (5.5)            |
| s0.3     | -0.32           | 0.15 (5.1)            | 0.034 (7.4)           |
| s1       | -0.50           | 0.05 (6.9)            | 0.014 (8.3)           |

Table 2. Observational Data

| Star         | Lit.<br>[Fe/H] | RNB<br>[Fe/H] | $T_{eff}$<br>(K) | RNB<br>[Li]      | RNB<br>EW(mA)  | T94<br>[Li]      | T94<br>EW(mA) |
|--------------|----------------|---------------|------------------|------------------|----------------|------------------|---------------|
| LP 651-4     | -2.96          | -2.60         | $6240 \pm 30$    | $2.11 \pm 0.039$ | $19.6 \pm 1.6$ | ...              | ...           |
| G4-37        | -2.73          | -2.70         | $6050 \pm 40$    | $2.11 \pm 0.045$ | $25.9 \pm 2.3$ | $2.08 \pm 0.083$ | $19 \pm 3.4$  |
| LP 831-7     | -3.25          | -3.32         | $6050 \pm 20$    | $2.07 \pm 0.029$ | $23.1 \pm 1.4$ | $2.18 \pm 0.051$ | $23 \pm 2.6$  |
| CD -331173   | -3.14          | -2.91         | $6250 \pm 20$    | $2.06 \pm 0.032$ | $17.2 \pm 1.2$ | $1.99 \pm 0.089$ | $12 \pm 2.4$  |
| BD +3 740    | -2.78          | -2.70         | $6240 \pm 40$    | $2.11 \pm 0.035$ | $19.5 \pm 1.1$ | $2.34 \pm 0.051$ | $24 \pm 2.4$  |
| BD +24 1676  | -2.71          | -2.38         | $6170 \pm 30$    | $2.10 \pm 0.047$ | $21.1 \pm 2.2$ | $2.37 \pm 0.049$ | $28 \pm 2.9$  |
| BD +20 2030  | -2.71          | -2.64         | $6200 \pm 40$    | $2.11 \pm 0.048$ | $20.5 \pm 2.0$ | $2.29 \pm 0.049$ | $23 \pm 2.2$  |
| BD +9 2190   | -2.89          | -2.83         | $6250 \pm 30$    | $2.00 \pm 0.042$ | $14.6 \pm 1.3$ | $2.19 \pm 0.085$ | $18 \pm 3.4$  |
| BD +1 2341p  | -2.82          | -2.79         | $6260 \pm 40$    | $2.09 \pm 0.046$ | $17.8 \pm 1.6$ | $2.34 \pm 0.057$ | $21 \pm 2.6$  |
| HD 84937     | -2.30          | -2.12         | $6160 \pm 30$    | $2.17 \pm 0.027$ | $24.9 \pm 1.1$ | $2.25 \pm 0.053$ | $22 \pm 2.5$  |
| BD -13 3442  | -2.99          | -2.79         | $6210 \pm 30$    | $2.12 \pm 0.034$ | $21.0 \pm 1.4$ | $2.42 \pm 0.053$ | $30 \pm 3.4$  |
| G 64-12      | -3.17          | -3.24         | $6220 \pm 30$    | $2.14 \pm 0.029$ | $21.2 \pm 1.1$ | $2.38 \pm 0.059$ | $28 \pm 3.6$  |
| G 64-37      | -3.23          | -3.15         | $6240 \pm 30$    | $2.09 \pm 0.040$ | $18.2 \pm 1.5$ | $2.06 \pm 0.054$ | $14 \pm 1.6$  |
| BD +26 2651  | -2.88          | ...           | $6150 \pm 40$    | $2.12 \pm 0.038$ | $22.5 \pm 1.5$ | $2.20 \pm 0.064$ | $20 \pm 2.9$  |
| CD -71 1234  | -2.50          | -2.60         | $6190 \pm 30$    | $2.20 \pm 0.025$ | $25.9 \pm 0.9$ | $2.36 \pm 0.051$ | $27 \pm 2.9$  |
| BD +26 3578  | -2.54          | -2.24         | $6150 \pm 40$    | $2.15 \pm 0.032$ | $24.6 \pm 1.1$ | ...              | ...           |
| LP 635-1     | -2.65          | -2.66         | $6270 \pm 30$    | $2.15 \pm 0.032$ | $20.2 \pm 1.2$ | $2.34 \pm 0.074$ | $24 \pm 3.9$  |
| LP 815-4     | -3.05          | -3.00         | $6340 \pm 30$    | $2.09 \pm 0.046$ | $16.1 \pm 1.6$ | $2.35 \pm 0.046$ | $22 \pm 2.1$  |
| CS 22943-095 | -2.55          | -2.20         | $6140 \pm 40$    | $2.12 \pm 0.035$ | $23.0 \pm 1.3$ | ...              | ...           |
| CD -35 14849 | -2.63          | -2.38         | $6060 \pm 20$    | $2.17 \pm 0.024$ | $28.8 \pm 1.4$ | ...              | ...           |
| G126-52      | -2.57          | -2.45         | $6210 \pm 40$    | $2.08 \pm 0.044$ | $19.1 \pm 1.6$ | $2.35 \pm 0.066$ | $26 \pm 3.6$  |
| CD -24 17504 | -3.55          | -3.24         | $6070 \pm 20$    | $1.97 \pm 0.033$ | $18.1 \pm 1.3$ | $2.15 \pm 0.072$ | $21 \pm 3.4$  |
| G186-26      | -2.85          | ...           | 6180             | ...              | ...            | $< 1.36$         | $< 2$         |

Table 3. Chemical Evolution Fits

| Case | $10^{10} L_i p$ | $10^{10}$ slope | Median [Li] | $\sigma(\text{pred})$ | $\sigma(\text{obs})$ |
|------|-----------------|-----------------|-------------|-----------------------|----------------------|
| HL   | $1.11 \pm 0.05$ | $97.5 \pm 24.7$ | 2.045       | 0.041                 | 0.046                |
| LL   | $1.17 \pm 0.05$ | $44.3 \pm 16.6$ | 2.065       | 0.039                 | 0.049                |
| HP   | $1.04 \pm 0.06$ | $21.4 \pm 5.0$  | 2.015       | 0.044                 | 0.048                |
| LP   | $1.12 \pm 0.06$ | $11.4 \pm 4.0$  | 2.05        | 0.039                 | 0.051                |
| HLno | $1.21 \pm 0.03$ | $56.8 \pm 17.0$ | 2.070       | 0.038                 | 0.045                |
| LLno | $1.22 \pm 0.03$ | $29.3 \pm 9.8$  | 2.080       | 0.037                 | 0.049                |
| HPno | $1.16 \pm 0.04$ | $12.8 \pm 3.6$  | 2.055       | 0.039                 | 0.046                |
| LPno | $1.19 \pm 0.04$ | $7.4 \pm 2.4$   | 2.065       | 0.038                 | 0.050                |

Table 4. Chemical Evolution Probabilities

| Case | Outlier Test |      |       | KS test |      |      |
|------|--------------|------|-------|---------|------|------|
|      | s0           | s0.3 | s1    | s0      | s0.3 | s1   |
| None | 0.45         | 0.15 | 0.05  | 0.49    | 0.13 | 0.06 |
| LL   | 0.31         | 0.11 | 0.04  | 0.32    | 0.15 | 0.05 |
| LP   | 0.38         | 0.15 | 0.06  | 0.52    | 0.18 | 0.04 |
| HL   | 0.38         | 0.13 | 0.045 | 0.34    | 0.14 | 0.03 |
| HP   | 0.35         | 0.12 | 0.04  | 0.66    | 0.19 | 0.06 |

Table 5. Inferred Primordial Lithium

| Case | Observed | s0   | s0.3 | s1   |
|------|----------|------|------|------|
| None | 2.11     | 2.29 | 2.43 | 2.61 |
| LL   | 2.07     | 2.25 | 2.39 | 2.57 |
| LP   | 2.05     | 2.23 | 2.37 | 2.55 |
| HL   | 2.05     | 2.23 | 2.37 | 2.55 |
| HP   | 2.02     | 2.20 | 2.34 | 2.52 |